Malaysian Journal of Analytical Sciences (MJAS)



Published by Malaysian Analytical Sciences Societ

EFFECTS OF *Pandanus amaryllifolius* LEAF EXTRACT CONCENTRATIONS ON THE MICROSTRUCTURAL PROPERTIES OF ZnO NANORODS VIA BIOLOGICALLY SYNTHESIZED ZnO SEED LAYER FORMATION

(Kesan Kepekatan Ekstrak *Pandanus amaryllifolius* Terhadap Ciri-Ciri Mikro dan Struktur Nanorod ZnO Melalui Pembentukan Lapisan Benih ZnO Bersifat Biologi)

Rabiatuladawiyah Md Akhir^{1,2*}, Irmaizatussyehdany Buniyamin^{2,1}, Kevin Alvin Eswar^{2,1,4}, Maryam Mohammad^{5,2,1}, Nurul Afaah Abdullah^{2,1}, Wan Marhaini Wan Harrum^{2,1}, Mohamad Rusop Mahmood^{2,3}, and Zuraida Khusaimi^{2,1*}

¹Faculty of Applied Sciences,
Universiti Teknologi MARA, 40450 Shah Alam, Selangor, Malaysia

²Centre for Functional Materials and Nanotechnology, Institute of Science,
Universiti Teknologi MARA, 40450 Shah Alam, Selangor, Malaysia

³NANO-Electronic Centre, Faculty of Electrical Engineering;
Universiti Teknologi MARA, 40450 Shah Alam, Selangor, Malaysia

⁴Faculty of Applied Sciences,
Universiti Teknologi MARA, Sabah Branch, Tawau Campus, 91032 Tawau, Malaysia

⁵Faculty of Applied Sciences,
Universiti Teknologi MARA, Perak Branch, Tapah Campus, Tapah Road, 35400, Perak, Malaysia

*Corresponding author: rabiatul9581@uitm.edu.my, zurai142@uitm.edu.my

Received: 13 September 2023; Accepted: 13 May 2024; Published: 27 August 2024

Abstract

An integrated strategy of spin-coating and solution immersion methods was carried out to produce well-aligned zinc oxide nanorods (ZnO NRs). First, a biologically synthesized ZnO seed layer (B-ZnO SL) solution was prepared using zinc nitrate hexahydrate as a precursor added with *Pandanus amaryllifolius* (PA) leaf extract at different concentrations (3% w/v, 6% w/v, and 9% w/v) as a stabilizer. This B-ZnO SL solution was deposited on a glass substrate using the spin-coating method. Second, ZnO-HMTA solution was prepared using zinc nitrate hexahydrate and hexamethylenetetramine (HMTA) as a precursor and stabilizer, respectively. This ZnO-HMTA solution was deposited onto the previously prepared B-ZnO SL. The optimum PA leaf extract concentration for enhanced ZnO NRs was determined by measuring the absorbance of B-ZnO SL via ultraviolet–visible analysis. The highest absorbance corresponded to B-ZnO SL that consisted of 6% w/v of PA leaf extract with an absorption peak of 375 nm. Using X-ray diffraction, three primary peaks for ZnO NRs were detected at $2\theta = 31.77^{\circ}$, 34.42° , and 36.24° , corresponding to (100), (002), and (101) ZnO crystallographic planes, respectively. By using field emission scanning electron microscopy, the smallest diameter of 96 nm was measured for the ZnO NRs synthesized on the B-ZnO SL with 6% w/v PA leaf extract. This study is the first to report on the efficacy of PA leaf extract at different concentrations to investigate the development of a highly crystalline and dense ZnO NRs structure.

Keywords: zinc oxide, nanorods, plant extract, spin-coating, solution immersion

Abstrak

Satu strategi bersepadu kaedah lapis-putar dan perendaman larutan telah dilakukan untuk menghasilkan nanorod zink oksida yang

Md Akhir et al.: EFFECTS OF Pandanus amaryllifolius LEAF EXTRACT CONCENTRATIONS ON THE MICROSTRUCTURAL PROPERTIES OF ZnO NANORODS VIA BIOLOGICALLY SYNTHESIZED ZnO SEED LAYER FORMATION

teratur (ZnO NRs). Pertama, larutan lapisan benih ZnO yang dihasilkan secara biologi (B-ZnO SL) disediakan menggunakan zink nitrat heksahidrat sebagai perintis dan ditambah ekstrak daun Pandanus amaryllifolius (PA) pada kepekatan berbeza (3% w/v, 6% w/v, dan 9% w/v) sebagai penstabil. Larutan B-ZnO SL ini telah dimendapkan pada substrat kaca menggunakan kaedah lapis-putar. Kedua, larutan ZnO-HMTA disediakan menggunakan zink nitrat heksahidrat dan heksametilenatetramina (HMTA) masing-masing sebagai perintis dan penstabil. Larutan ZnO-HMTA ini dimendapkan ke atas B-ZnO SL yang disediakan sebelumnya. Kepekatan ekstrak daun PA yang optimum bagi peningkatan ciri-ciri ZnO NRs ditentukan dengan mengukur serapan B-ZnO SL melalui analisis ultralembayung-tampak. Serapan tertinggi yang diperoleh selaras dengan B-ZnO SL yang mengandungi 6% w/v ekstrak daun PA pada puncak serapan 375 nm. Dengan menggunakan belauan sinar-X, tiga puncak utama ZnO NRs dikesan pada 20 = 31.78°, 34.47°, dan 36.26°, masing-masing sejajar dengan satah kristalografi ZnO (100), (002), dan (101). Dengan menggunakan mikroskopi elektron pengimbasan pancaran medan, diameter terkecil 96 nm diukur bagi ZnO NRs yang dihasilkan di atas B-ZnO SL dengan 6% w/v ekstrak daun PA. Kajian ini adalah yang pertama melaporkan keberkesanan ekstrak daun PA pada kepekatan yang berbeza untuk mengkaji perkembangan struktur ZnO NRs yang sangat berhablur dan padat.

Kata kunci: zink oksida, nanorod, ekstrak tumbuhan, lapis-putar, perendaman larutan

Introduction

Oriented zinc oxide nanorods (ZnO NRs) are particularly remarkable among diverse nanostructures due to their elevated levels of crystallinity, well-defined density of states, efficient one-dimensional charge transport, and substantial specific surface area. These render them highly applicable implementation in semiconductor devices and various other optoelectronic applications. While nanostructured ZnO is typically nontoxic, the synthesis process utilizes solvents or chemicals with moderate to high toxicity [1-3]. Hence, researchers are using a more eco-sustainable approach, such as solution immersion technique [4-5]. This method mainly uses monoethanolamine (MEA) or hexamethylenetetramine (HMTA) as a stabilizer to produce nanostructured ZnO such as ZnO NRs. Using this approach prevents the aggregation of the precursor solution [6-8]. As the eco-sustainable approach has plant-mediated toward synthesis, achievements to date and prospects of a plant-mediated method to produce nanostructured ZnO have been summarized in several reports [9-11]. In recent years, comparable rod-shaped nanostructured ZnO has been synthesized using leaf extract [12-16]. However, it is still challenging to produce consistent ZnO NRs using this strategy, especially via single-step synthesis as reported in earlier research [17]. The primary objective of this study is to synthesize oriented, well-aligned ZnO NRs with improved crystallinity via biologically synthesized ZnO seed layer (B-ZnO SL) formation. This was accomplished via an integrated strategy of spincoating and solution immersion methods. Pandanus (PA) leaf extract at different amaryllifolius concentrations were used to prepare B-ZnO SL via spincoating method. The optimum B-ZnO SL was determined by UV-vis analysis. The microstructure of B-ZnO SL was also investigated using FESEM to correlate the efficacy of PA leaf extract concentrations during B-ZnO SL preparation with the development of oriented and well-aligned ZnO NRs. Our study anticipates that the incorporation of B-ZnO SL will substantially enhance the structural and morphological characteristics of ZnO NRs.

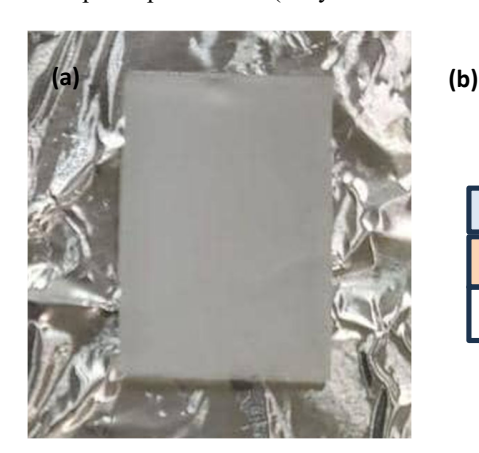
Materials and Methods

To achieve the study objectives, the methodology was separated into several stages: (1) Preparation of glass substrate, (2) i) Preparation of B-ZnO SL solution, ii) Deposition of B-ZnO SL solution onto a cleaned glass substrate via spin-coating method, (3) i) Preparation of ZnO-HMTA solution, ii) Deposition of ZnO-HMTA solution onto B-ZnO SL via solution immersion method. The resulting ZnO NRs on B-ZnO SL (top view) is shown in Figure 1 (a) while Figure 1 (b) illustrates the schematic diagram of the cross-sectional area of sample.

The glass preparation stage is critical for successfully synthesizing refined crystalline and well-aligned ZnO NRs. The B-ZnO SL solution was prepared using 0.1 M zinc nitrate hexahydrate [Zn(NO₃)₂·6H₂O] as a precursor with PA leaf extract at concentrations of 3% w/v, 6% w/v, and 9% w/v as a stabilizer. The solution was mixed based on the standard procedure as described elsewhere [17,18-19]. By using the spin-coating method, 10 drops of the prepared solution were deposited on the glass substrate at 3000 rpm for 30 s. Then, the deposited ZnO seed layer was preheated at 150 °C for 10 min. The procedure was repeated five times to produce 5 seed

layers of ZnO. After the spin-coating process, the deposited ZnO seed layer was annealed at 450 °C for 1 h. Next, equimolar ZnO-HMTA solution was prepared using Zn(NO₃)₂·6H₂O and HMTA at 0.1 M as a precursor and stabilizer, respectively. The solution mixing process was performed as described elsewhere [17-19]. The optical properties of B-ZnO SL synthesized using different PA leaf extract concentrations were determined using a UV-vis spectrophotometer (Cary 60

UV-Vis). The morphologies of optimum B-ZnO SL and ZnO NRs were observed using field emission electron scanning microscopy (FESEM; JEOL JSM 7600F), while the phase and crystal structure of ZnO NRs were assessed by using X-ray diffraction (XRD; PANalytical X'Pert Powder). Finally, energy-dispersive X-ray (EDX) analysis was done to confirm the presence of zinc and oxygen.



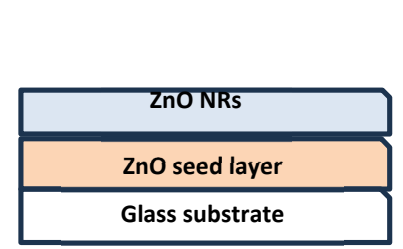


Figure 1. (a) Top view, (b) schematic diagram of cross section view of ZnO NRs deposited onto B-ZnO SL

The glass preparation stage is critical for successfully synthesizing refined crystalline and well-aligned ZnO NRs. The B-ZnO SL solution was prepared using 0.1 M zinc nitrate hexahydrate [Zn(NO₃)₂·6H₂O] as a precursor with PA leaf extract at concentrations of 3% w/v, 6% w/v, and 9% w/v as a stabilizer. The solution was mixed based on the standard procedure as described elsewhere [17,18-19]. By using the spin-coating method, 10 drops of the prepared solution were deposited on the glass substrate at 3000 rpm for 30 s. Then, the deposited ZnO seed layer was preheated at 150 °C for 10 min. The procedure was repeated five times to produce 5 seed layers of ZnO. After the spin-coating process, the deposited ZnO seed layer was annealed at 450 °C for 1 h. Next, equimolar ZnO-HMTA solution was prepared using Zn(NO₃)₂·6H₂O and HMTA at 0.1 M as a precursor and stabilizer, respectively. The solution mixing process was performed as described elsewhere [17-19]. The optical properties of B-ZnO SL synthesized using different PA leaf extract concentrations were determined using a UV-vis spectrophotometer (Cary 60 UV-Vis). The morphologies of optimum B-ZnO SL and ZnO NRs were observed using field emission electron scanning microscopy (FESEM; JEOL JSM 7600F), while the phase and crystal structure of ZnO NRs were

assessed by using X-ray diffraction (XRD; PANalytical X'Pert Powder). Finally, energy-dispersive X-ray (EDX) analysis was done to confirm the presence of zinc and oxygen.

Results and Discussion Optical properties of B-ZnO SL

The optical properties of B-ZnO SL synthesized with different PA leaf extract concentrations as a stabilizer are shown in Figure 2. The absorption peak centered at *375 nm is the characteristic peak for hexagonal wurtzite ZnO, which is the same pattern obtained from previous research [20-22]. The absorption peak shows a red shift compared to that of bulk ZnO (365 nm) [23]. This red shift can be attributed to the development of shallow levels inside the band gap due to the presence of foreign atoms in the lattice [24,25]. The absorbance of the ZnO seed layer increased as PA leaf extract concentration was increased to 6%. The use of PA leaf extract as a stabilizer in the ZnO seed layer might have provided more flavonoid compounds, as evidenced by the increase in UV absorption compared to the control sample (0% PA). The optimum PA leaf extract concentration as a stabilizer was determined to be 6% w/v based on the UV-vis finding.

Md Akhir et al.: EFFECTS OF *Pandanus amaryllifolius* LEAF EXTRACT CONCENTRATIONS ON THE MICROSTRUCTURAL PROPERTIES OF ZnO NANORODS VIA BIOLOGICALLY SYNTHESIZED ZnO SEED LAYER FORMATION

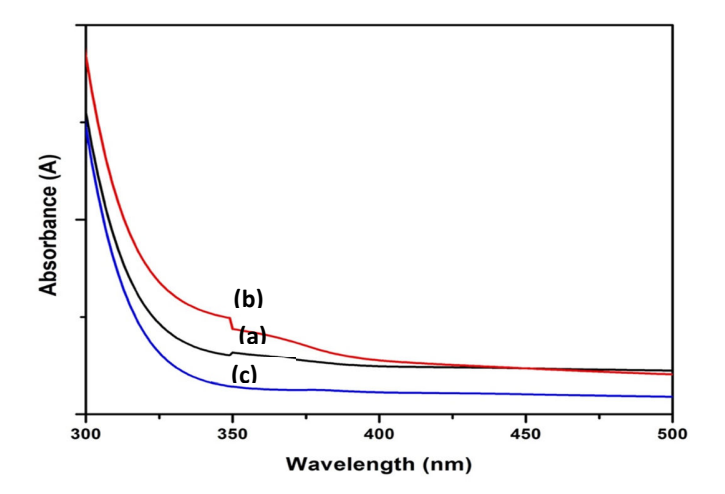


Figure 2. Absorbance of B-ZnO SL synthesized using PA leaf extract with concentrations of (a) 3% w/v, (b) 6% w/v, and (c) 9% w/v

Morphological properties of B-ZnO SL

The morphology of B-ZnO SL synthesized with 6% w/v PA leaf extract was studied and compared with that of the ZnO seed layer at which 0% w/v of PA was utilized (control sample). The B-ZnO SL thin film prepared with 6% PA leaf extract has a spongelike, porous morphology, as shown in Figure 3 (b). Laurenti and Cauda described this morphology as a porous nanobranched structure with a high specific surface area [26]. With a high specific surface area, the porous B-ZnO SL provides high energy for the formation of wellaligned nanorod structures. The particles had an average size in the range of 8-10 nm. In comparison, the ZnO seed layer thin film prepared using 0% PA leaf extract (Figure 2 (a)) has a slightly bigger particle size (12.38 nm). The 0% PA sample also consisted of many aggregates. Poor colloidal stability of nanoparticles in fluid may cause aggregation [27,28]. ZnO nanoparticles also have a high tendency to aggregate which may lower the surface energy. As aggregates become larger and denser with strong bonds, the surface reactivity decreases. The utilization of 6% PA as a stabilizer in B-ZnO SL provided more biomolecules such as flavonoid compounds. These compounds act as a stabilizing agent that resulted in homogeneous ZnO nanoparticles compared to the control sample.

Microstructural properties of ZnO NRs

The orientation of ZnO NRs significantly changed when 784

PA leaf extract concentration was varied when preparing the B-ZnO SL growth solution. This is evidenced by the increase in UV-vis absorbance as PA leaf extract concentration was increased (Figure 2). UV-vis absorbance was related with the flavonoid compounds in the PA leaf extract, which were responsible in coordinating and stabilizing the ZnO nanoparticles within B-ZnO SL. This directly impacted the overall microstructural properties of ZnO NRs (Figures 4 & 5). The samples exhibit significant diffraction peaks (Figure 4), indicating a comparable enhanced crystallinity to ZnO NRs synthesized via the integrated approach used in this study. Furthermore, the absence of other peaks suggests no contaminants in the sample. This XRD pattern is known as the hexagonal wurtzite structure (JCPDS No. 36-1451). The three peaks at $2\theta = 31.77^{\circ}$, 34.42°, and 36.24° correlate to the (100), (002), and (101) crystalline planes of ZnO, respectively. These three dominant peaks are consistent with those found in earlier research using hydrothermal [29] and sol-gel immersion processes [30]. As PA leaf extract concentration was increased during the preparation of B-ZnO SL, the peak intensity of ZnO NRs in XRD data also increased. The intensity or the count numbers can be assigned as the relative crystallinity of the sample. The decrease in ZnO NRs crystallinity when 9% w/v of PA leaf extract was used can be explained by the excessive amount of biomolecule compounds present in the B-ZnO SL solution. Instead of stabilizing the Zn and

O atoms, this excessive stabilizing agent was no longer efficient, producing lower ZnO purity [31]. In addition, the ZnO NRs synthesized in this study showed a superior purity as only three prominent peaks appeared in XRD, compared with the rod-shaped ZnO synthesized in a previous study [32].

The synthesized ZnO NRs (Figure 5 (a)) had a rodlike structure with irregular orientation as shown by the FESEM images in Figure 5 (a). This structure caused a bent or tilted configuration when the NRs were deposited onto the B-ZnO SL at 0% PA leaf extract (control sample). Utilizing different PA leaf extract concentrations as stabilizers during the preparation of the B-ZnO SL yielded distinct properties in terms of rod structure orientation and the diameter of the final deposited ZnO NRs. The smallest diameter of ZnO NRs measured was approximately 96 nm. The smaller diameter size and the uniformity of ZnO NRs when

deposited onto B-ZnO SL (6% w/v) can be correlated with a synergistic effect between the increase in crystallinity as evident in Figure 4 (b). This is also further supported by the prominent (002) peak observed in the XRD data. This is due to the presence of dense ZnO nanoparticles with lower number of aggregates as shown in Figure 3 (b). With lower number of aggregates, more energy was directed to coordinate the Zn and O efficiently in the ZnO NRs. This facilitates the vertically aligned ZnO NRs perpendicular to the substrate as evident in Figure 5 (c). These findings show a remarkable microstructural improvement compared to previous rod-shaped ZnO fabricated via other biosynthesis routes [33]. EDX was conducted to further evidence the presence of elemental zinc and oxygen in ZnO NRs, and the result is shown in Figure 6. Only Zn and O atoms were detected, confirming a high purity of the prepared ZnO.

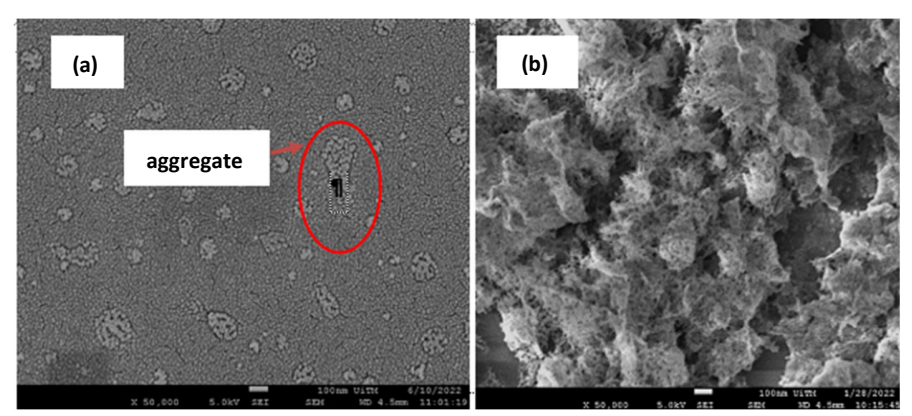


Figure 3. FESEM images of B-ZnO SL synthesized with (a) 0% and (b) 6% w/v PA leaf extract

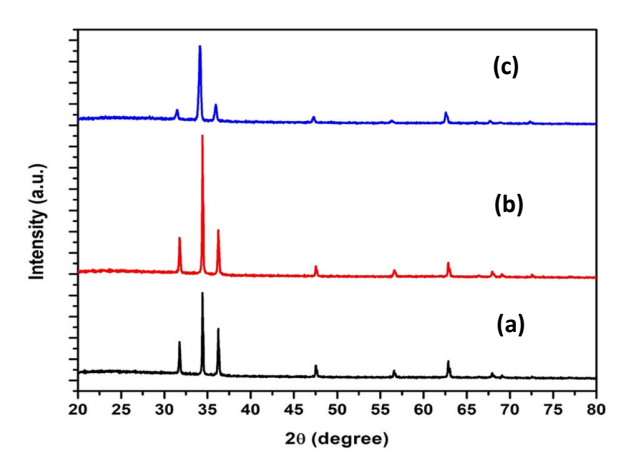


Figure 4. XRD pattern of ZnO NRs deposited onto B-ZnO SL synthesized with PA leaf extract concentrations of (a) 3% w/v, (b) 6% w/v, and (c) 9% w/v

Md Akhir et al.: EFFECTS OF *Pandanus amaryllifolius* LEAF EXTRACT CONCENTRATIONS ON THE MICROSTRUCTURAL PROPERTIES OF ZnO NANORODS VIA BIOLOGICALLY SYNTHESIZED ZnO SEED LAYER FORMATION

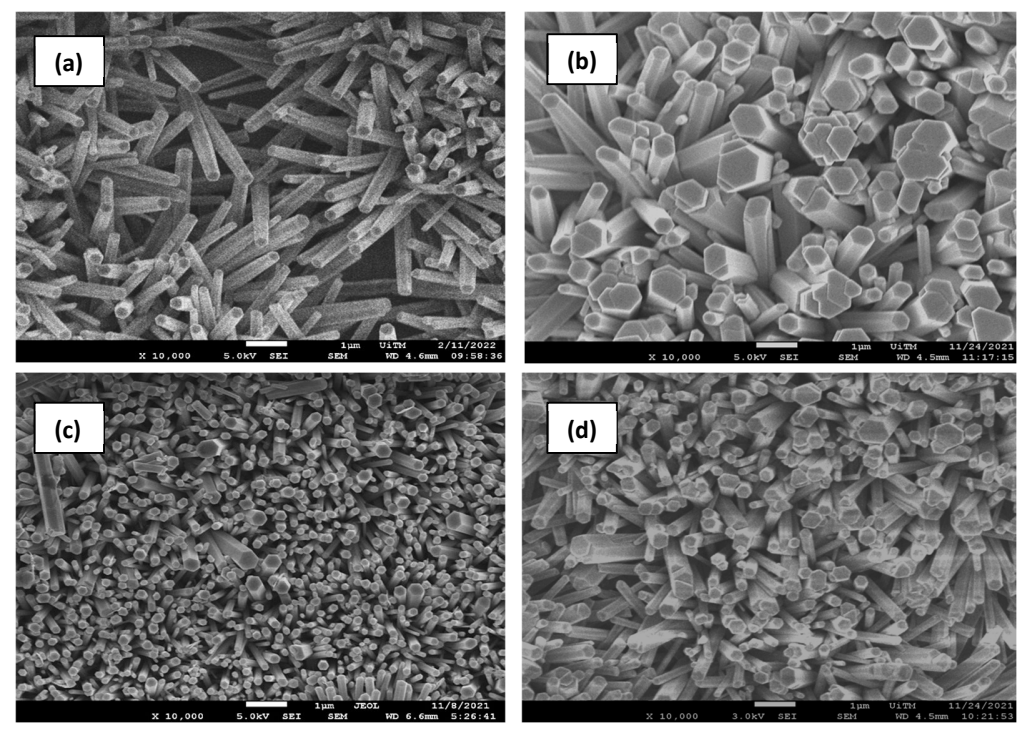


Figure 5. FESEM images of ZnO NRs deposited onto B-ZnO SL synthesized with PA leaf extract concentrations of (a) 0% w/v, (b) 3% w/v, (c) 6% w/v, and (d) 9% w/v

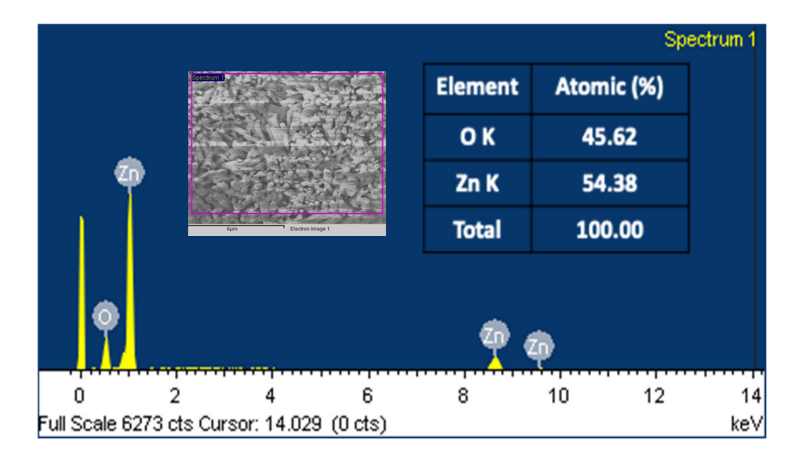


Figure 6. EDX data of ZnO NRs deposited onto B-ZnO SL synthesized with 6% w/v PA leaf extract

Conclusion

ZnO NRs were successfully prepared on a B-ZnO SL synthesized with PA leaf extract. The optimum PA leaf extract concentration was 6% w/v, at which the highest absorbance of the corresponding B-ZnO SL was obtained. The improved absorbance was attributed to the relatively higher amount of flavonoid compounds present in the corresponding sample. The crystallinity of

the ZnO NRs improved for the sample deposited on B-ZnO SL prepared with 6% w/v PA leaf extract, with a dominant peak of the (002) orientation compared to the samples deposited on seed layers prepared with other concentrations. The average diameter of the ZnO NRs was 96 nm as shown through FESEM analysis, which is a 70% reduction from the control sample. The significant diameter reduction together with improved

vertical alignment of ZnO NRs may benefit their application for conductive electrodes and UV or humidity sensors. Subsequent studies should include a detailed analysis of other synergistic parameters to arrive at a comprehensive conclusion.

Acknowledgement

This work was supported by the Centre for Functional Materials and Nanotechnology, Institute of Science, Universiti Teknologi MARA. The authors also gratefully acknowledge the Faculty of Applied Sciences, Universiti Teknologi MARA for providing the research facilities. Special thanks to Ts. Salifairus Mohammad Jafar (UiTM Senior Science Officer), En. Mohd Azlan Jaafar (UiTM Assistant Engineer), Puan Nurfarah Farini Muhamad Kamarazzaman (UiTM Assistant Science Officer), and Puan Hasdiyana Hashim (UiTM Science Officer) for their help and kind support to this research.

References

- 1. Czyżowska, A., & Barbasz, A. (2022). A review: zinc oxide nanoparticles–friends or enemies?. *International Journal of Environmental Health Research*, 32(4): 885-901.
- Verma, R., Pathak, S., Srivastava, A. K., Prawer, S., and Tomljenovic-Hanic, S. (2021). ZnO nanomaterials: Green synthesis, toxicity evaluation and new insights in biomedical applications. *Journal of Alloys and Compounds*, 876: 160175.
- Naveed Ul Haq, A., Nadhman, A., Ullah, I., Mustafa, G., Yasinzai, M., and Khan, I. (2017). Synthesis approaches of zinc oxide nanoparticles: the dilemma of ecotoxicity. *Journal of Nanomaterials*, 2017: 510342.
- 4. Akhir, R. M., Harrum, W. M. W., Buniyamin, I., Rusop, M., and Khusaimi, Z. (2022). Enhanced structural and morphological properties of ZnO nanorods using plant extract-assisted solution immersion method. *Materials Today: Proceedings*, 48: 1855-1860.
- Harrum, W. M. W., Akhir, R. M., Afaah, A. N., Eswar, K. A., Husairi, F. S., Rusop, M., and Khusaimi, Z. (2022). Comparative study of surface, elemental, structural and optical morphologies of titanium dioxide-zinc oxide (TiO₂-ZnO) and titanium dioxide-zinc oxide/graphene (TiO₂-ZnO/Gn). *Materials Today: Proceedings*, 75: 147-150.
- 6. Factori, I. M., Amaral, J. M., Camani, P. H., Rosa,

- D. S., Lima, B. A., Brocchi, M., ... and Souza, J. S. (2021). ZnO nanoparticle/poly (vinyl alcohol) nanocomposites via microwave-assisted sol–gel synthesis for structural materials, UV shielding, and antimicrobial activity. *ACS Applied Nano Materials*, 4(7): 7371-7383.
- Methaapanon, R., Chutchakul, K., and Pavarajarn, V. (2020). Photocatalytic zinc oxide on flexible polyacrylonitrile nanofibers via sol–gel coaxial electrospinning. *Ceramics International*, 46(6): 8287-8292.
- 8. Badnore, A.U. and Pandit, A.B. (2017). Effect of pH on sonication assisted synthesis of ZnO nanostructures: process details. *Chemical Engineering and Processing: Process Intensification*, 122: 235-244.
- Akintelu, S. A., and Folorunso, A. S. (2020). A review on green synthesis of zinc oxide nanoparticles using plant extracts and its biomedical applications. *BioNanoScience*, 10(4): 848-863.
- Bandeira, M., Giovanela, M., Roesch-Ely, M., Devine, D. M., and da Silva Crespo, J. (2020). Green synthesis of zinc oxide nanoparticles: A review of the synthesis methodology and mechanism of formation. Sustainable Chemistry and Pharmacy, 15: 100223.
- 11. Vishnukumar, P., Vivekanandhan, S., Misra, M. and Mohanty, A. K. (2018). Recent advances and emerging opportunities in phytochemical synthesis of ZnO nanostructures. *Materials Science in Semiconductor Processing*, 80: 143-161.
- 12. Jeevanandam, Y, San Chan, and Ku, Y. H. (2018). Aqueous *Eucalyptus globulus* leaf extract-mediated biosynthesis of MgO nanorods. *Applied Biological Chemistry*, 61(2): 197-208.
- Rani, N., Saini, M., Yadav, S., Gupta, K., Saini, K., and Khanuja, M. (2020, October). High performance super-capacitor based on rod shaped ZnO nanostructure electrode. In *AIP Conference Proceedings* (Vol. 2276, No. 1, p. 020042). AIP Publishing LLC.
- 14. Dejen, K. D., Zereffa, E. A., Murthy, H. A., and Merga, A. (2020). Synthesis of ZnO and ZnO/PVA nanocomposite using aqueous *Moringa oleifeira* leaf extract template: antibacterial and electrochemical activities. *Reviews on Advanced Materials Science*, 59(1): 464-476.
- Hassan Basri, H., Talib, R. A., Sukor, R., Othman,
 H., and Ariffin, H. (2020). Effect of synthesis

- temperature on the size of ZnO nanoparticles derived from pineapple peel extract and antibacterial activity of ZnO–starch nanocomposite films. *Nanomaterials*, 10(6): 1061.
- Rani, N., Rawat, K., Saini, M., Yadav, S., Shrivastava, A., Saini, K., and Maity, D. (2022). *Azadirachta indica* leaf extract mediated biosynthesized rod-shaped zinc oxide nanoparticles for in vitro lung cancer treatment. *Materials Science* and Engineering: B, 284: 115851.
- 17. Akhir, R. M., Harrum, W. M. W., Buniyamin, I., Rusop, M., and Khusaimi, Z. (2022). Enhanced structural and morphological properties of ZnO nanorods using plant extract-assisted solution immersion method. *Materials Today: Proceedings*, 48: 1855-1860.
- Akhir, R. M., Umbaidilah, S. Z., Abdullah, N. A., Buniyamin, I., Rusop, M., and Khusaimi, Z. (2021). Comparative study on morphology, structural and optical properties of non-seeded and seeded ZnO nanorods. In *Recent Trends in Manufacturing and Materials Towards Industry 4.0: Selected Articles from iM3F 2020, Malaysia* (pp. 961-969). Springer Singapore.
- 19. Md Akhir, R., Umbaidilah, S. Z., Abdullah, N. A., Alrokayan, S. A., Khan, H. A., Soga, T., ... and Khusaimi, Z. (2020). The potential of pandanus amaryllifolius leaves extract in fabrication of dense and uniform ZnO microrods. *Micromachines*, 11(3): 299.
- Mahajan, P., Singh, A., and Arya, S. (2020). Improved performance of solution processed organic solar cells with an additive layer of sol-gel synthesized ZnO/CuO core/shell nanoparticles. *Journal of Alloys and Compounds*, 814: 152292.
- Hasabeldaim, E., Ntwaeaborwa, O. M., Kroon, R. E., and Swart, H. C. (2019). Structural, optical and photoluminescence properties of Eu doped ZnO thin films prepared by spin coating. *Journal of Molecular Structure*, 1192: 105-114.
- 22. Xu, L., Miao, J., Chen, Y., Su, J., Yang, M., Zhang, L., ... and Ding, S. (2018). Characterization of Agdoped ZnO thin film for its potential applications in optoelectronic devices. *Optik*, 170: 484-491.
- 23. Sun, J. H., Dong, S. Y., Feng, J. L., Yin, X. J., and Zhao, X. C. (2011). Enhanced sunlight photocatalytic performance of Sn-doped ZnO for

- Methylene Blue degradation. *Journal of Molecular Catalysis A: Chemical*, 335(1-2): 145-150.
- Reddy, A. J., Kokila, M. K., Nagabhushana, H., Rao, J. L., Shivakumara, C., Nagabhushana, B. M., and Chakradhar, R. P. S. (2011). Combustion synthesis, characterization and Raman studies of ZnO nanopowders. Spectrochimica Acta Part A: Molecular and Biomolecular Spectroscopy, 81(1): 53-58.
- Misra, K. P., Kumawat, A., Kumari, P., Samanta, S., Halder, N., and Chattopadhyay, S. (2021). Band gap reduction and petal-like nanostructure formation in heavily Ce-doped ZnO nanopowders. *Journal of Nano-and Electronic Physics*, 13(2).
- Laurenti, M., and Cauda, V. (2018). Porous zinc oxide thin films: Synthesis approaches and applications. *Coatings*, 8(2): 67.
- 27. Chai, M. H. H., Amir, N., Yahya, N., and Saaid, I. M. (2018). Characterization and colloidal stability of surface modified zinc oxide nanoparticle. In *Journal of Physics: Conference Series* (Vol. 1123, No. 1, p. 012007). IOP Publishing.
- Shrestha, S., Wang, B., and Dutta, P. (2020). Nanoparticle processing: Understanding and controlling aggregation. Advances in Colloid and Interface Science, 279: 102162.
- Rajamanickam, S., Mohammad, S. M., and Hassan,
 Z. (2020). Effect of zinc acetate dihydrate concentration on morphology of ZnO seed layer and
 ZnO nanorods grown by hydrothermal method.
 Colloid and Interface Science Communications, 38: 100312.
- Ameer, A. A., Suriani, A. B., Jabur, A. R., Hashim, N., and Zaid, K. (2019). The fabrication of zinc oxide nanorods and nanowires by solgel immersion methods. In *Journal of Physics: Conference Series* (Vol. 1170, No. 1, p. 012005). IOP Publishing.
- Ruangtong, J., Jiraroj, T., and T-Thienprasert, N. P. (2020). Green synthesized ZnO nanosheets from banana peel extract possess anti-bacterial activity and anti-cancer activity. *Materials Today Communications*, 24: 101224.
- 32. Khatami, M., Khatami, S., Mosazade, F., Raisi, M., Haghighat, M., Sabaghan, M., ... and Varma, R. S. (2020). Greener synthesis of rod shaped zinc oxide nanoparticles using *Lilium ledebourii* tuber and evaluation of their leishmanicidal activity. *Iranian*

Journal of Biotechnology, 18(1): e2196.

Chennimalai, M., Do, J. Y., Kang, M., and Senthil,
 T. S. (2019). A facile green approach of ZnO NRs

synthesized via *Ricinus communis* L. leaf extract for biological activities. *Materials Science and Engineering: C*, 103: 109844.